CONF-961202--11 SAND96-1714C

INTERACTION OF CAVITIES AND DISLOCATIONS IN SEMICONDUCTORS

D. M. FOLLSTAEDT, S. M. MYERS, S. R. LEE, J. L. RENO, R. L. DAWSON and J. HAN
Sandia National Laboratories, Albuquerque, NM 87185-1056 (dmfolls@sandia.gov)

ABSTRACT

Transmission electron microscopy of He-implanted Si-Ge and InGaAs indicates an attractive interaction between cavities and dislocations. Calculation indicates that cavities are attracted to dislocations through surrounding strain fields, and strong binding (100s of eV) occurs when a cavity intersects the core. In a strained SiGe/Si heterostructure, He implantation enhances relaxation rates and cavities bound to misfit dislocations show evidence of increasing relaxation at equilibrium by lowering dislocation energies. The interaction is expected for all crystalline solids, and gives insight into voids in GaN/sapphire and bubbles in He-implanted metals.

INTRODUCTION TO CAVITY-DISLOCATION INTERACTIONS

Ion implantation of insoluble gases into solids leads to formation of bubbles that enlarge when there is sufficient atomic mobility. For some semiconductors [1-3], subsequent anneals can degas He, leaving empty cavities. We have found recently [4,5] that cavities bind strongly to dislocations in Si-Ge materials. Here we discuss the nature and magnitude of this interaction. We show that implanting He at the interface of strained SiGe/Si heterostructures increases the relaxation rate during annealing, and that the resulting cavities bind to misfit dislocations, which appears to produce a greater degree of strain relaxation than in the absence of cavities. Binding of cavities to dislocations is also demonstrated in an InGaAs/GaAs heterostructure, and is used to explain microstructures of tubular voids in GaN grown on sapphire and He bubbles in metals.

The attractive interaction is demonstrated in Ge by the transmission electron microscopy (TEM) image in Fig. 1. A dose of $1x10^{17}$ He/cm^2 was implanted at 50 keV and the material was annealed 1 hr. at 700°C. This anneal produced significant atomic mobility in Ge, allowing the cavities to coarsen to an average diameter of 60 nm and the microstructure to evolve toward low energy configurations. The dislocation segments extend directly from cavity to cavity and often intersect their surfaces nearly orthogonally, which maximizes the intersected length. We use such images as evidence for an interaction between cavities and dislocations, but a detailed explanation of microstructural evolution during annealing is beyond the scope of this paper.

Theoretical treatment of cavities near a dislocation shows an attractive interaction through the strain fields surrounding the dislocation, and a strong binding when the cavity intersects the dislocation core. Elastic continuum theory was first applied to selected cases of cavities in strain fields where analytical solutions are obtainable, including a spherical void in a hydrostatically compressed solid and a long cylindrical void parallel to a screw dislocation [6]. These solutions indicate that the strain energy reduction upon moving a void into an elastically deformed region is ~1.5-2.0 times the energy initially present in the volume of the void. The small size of this correction indicates that strain fields around the cavity are significantly modified for only a short distance beyond it. This result was used to approximate solutions of complex configurations by integrating the initial dislocation strain energy over the volume of the void and multiplying by 2. To treat the interaction when the cavity intersects the core, we use the accepted practice of truncating the integral of strain energy at a radius $r_o = b/4$, where b is the Burger's vector [7*].

A spherical void next to a dislocation is of basic interest. The binding energy calculated from the strain fields around a screw dislocation in Si is given in Fig. 2 as a function of distance (R_{dis})

DISCLAIMER

DISCLAIMER

Portions of this document may be illegible in electronic image products. Images are produced from the best available original document.

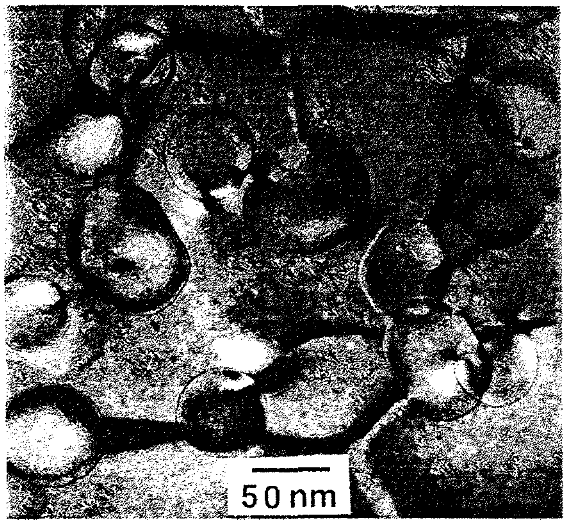

Figure 1. Dislocations intersecting cavities in Ge.

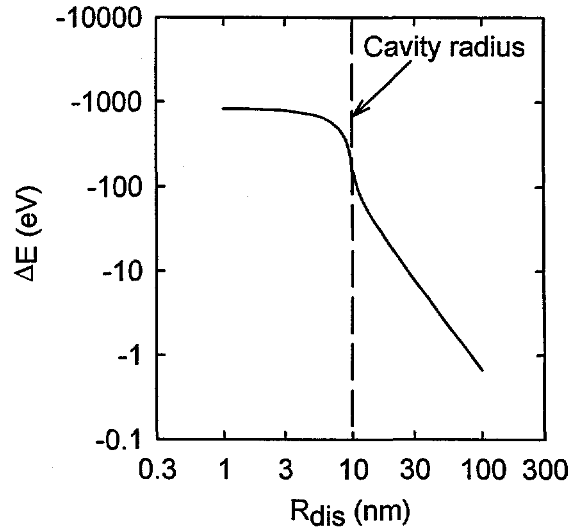

Figure 2. Calculated binding of 10 nm-radius cavity to screw dislocation in Si.

from the core to the center of a 10 nm-radius cavity. At R_{dis} = 20 nm this energy is 19 eV; the binding increases rapidly as the cavity edge nears the core and reaches ~800 eV when the cavity is centered on the core. At greater distance the energy falls as $1/R_{dis}^2$. Thus the attraction is very strong but of short range. Energy reductions of 100's of eV for cavities centered on dislocations explain the observation in Fig. 1 that these entities position to maximize intercepted core lengths.

SiGe/Si HETEROSTRUCTURES

To examine the influence of cavities on misfit dislocations, He^+ was implanted into a fully strained heterostructure of 140 nm of $Si_{0.86}Ge_{0.14}$ on (001) Si, grown by ultrahigh-vacuum chemical vapor deposition [7]. Implantation of 1.7×10^{16} He/cm^2 at 15 keV with the specimen tilted 30° from normal incidence and then annealing for 1 hour at 900°C produced a 60 nm-thick layer of cavities 10-30 nm in diameter at the interface, as seen in Fig. 3a. This implantation produced a peak concentration ≈1.6 at.% He, for which a thin cavity layer forms in Si [8].

Strain in the alloy layer was examined with x-ray diffraction. By using (004) and (224) reflections, both the normal and in-plane lattice constants of the alloy were determined, and the percentage change of the in-plane constant as compared to that needed to relax from the fully strained value of Si (0.5431 nm) to the unstrained alloy value (0.5459 nm) was derived. The specimen of Fig. 3a was relaxed by 54% (Table I), while an unimplanted reference remained almost fully strained after this anneal. The implantation damage and cavities at the interface probably provided numerous nucleation sites for misfit dislocations and thus enhanced the initial relaxation rate during annealing, as found for other implanted species [9]. With the cavity layer, dislocations remained closely confined to the interface, whereas they protruded into the substrate of the unimplanted reference [4]. This difference is consistent with dislocations binding to the cavity layer, but may also be due to the change in nucleation. For example, the modified Frank-Read mechanism expected for relaxation of homogeneous SiGe/Si heterostructures would produce dislocations extending into the substrate [10] and may have operated in the reference.

The microstructure in Fig. 3b resulted from implanting of 4×10^{16} He/cm^2 at 15 keV (no tilting) into the heterostructure and then annealing for 1 hour at 900°C. With this implant, higher He concentrations were present over a thicker depth interval and cavities formed in the overlayer as well as behind the interface. Cavities 3-20 nm in diameter lie in rows along dislocations within

50 nm below the interface. Cavities 20-55 nm in diameter are found in the overlayer as close as 20 nm to surface; their larger size reflects increased thermal evolution with the Ge content. Cavities in the alloy near the interface are especially large; very few small cavities are found in the layer or within ~10 nm below it. A void intersecting a strained layer will experience a force tending to move it into the layer in order to reduce the strain energy. Here, cavities once at the interface may have migrated into the overlayer and coalesced into the large cavities.

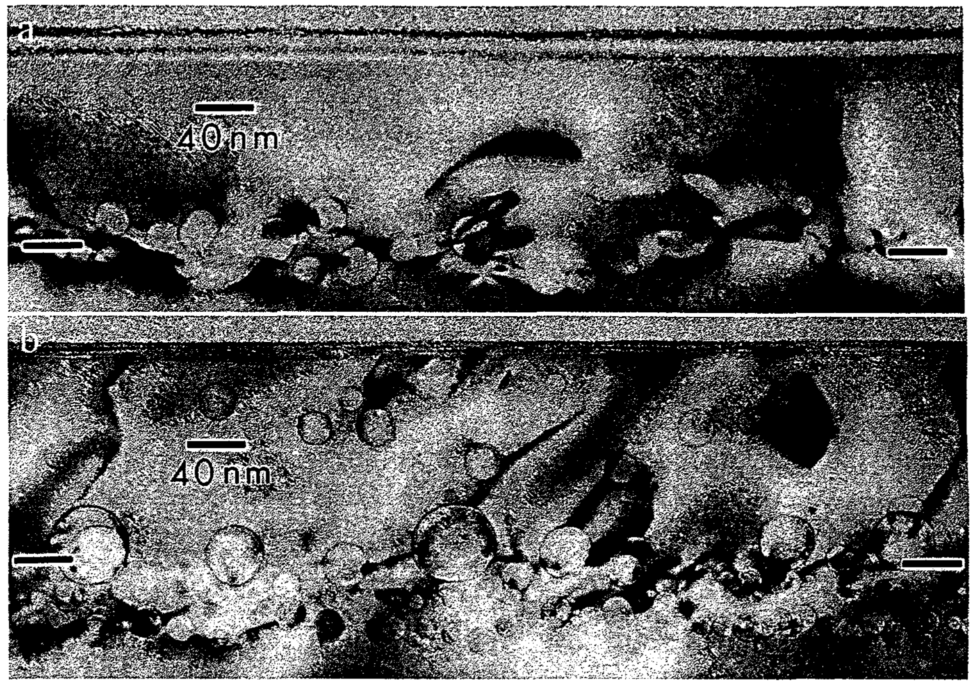

Figure 3. a) Cross-section TEM image of $Si_{0.86}Ge_{0.14}/Si$ implanted with $1.7x10^{16}$ He/cm^2 and annealed 1 hr. at 900°C. b) $4x10^{16}$ He/cm^2, same anneal.

Figure 3b also shows dislocations threading through the alloy, with most of them intersecting a large (~35 nm) cavity. Using the gradient of the energy in Fig. 2 to determine the force necessary to break a dislocation from a 20 nm-diameter cavity, we find it approximately equal to the driving force to propagate a threading segment attached to a misfit dislocation when this alloy is fully strained [11]. It appears unlikely that dislocations will break free from the large cavities in Fig 3b, especially after some strain relaxation has occurred. The intersection of threading dislocations with such cavities is thus expected to inhibit further relaxation by propagation of existing misfit dislocations. The high degree of relaxation achieved with this implanted structure (81%) is apparently due to the nucleation of additional dislocations.

To examine the interaction of cavities with misfit dislocations further [5], the alloy of Fig. 3a was back-thinned and examined in plan-view. In a sample region thick enough to contain the misfit dislocation network, weak-beam TEM images were obtained with the (220) reflection as in Fig. 4. Instead of a rectangular pattern of straight misfit dislocations extending for several micrometers as in other heterostructures, a network of short dislocation segments ~100 nm long is seen, whose cores (illuminated in Fig. 4) intersect cavities and change directions often. The misfit dislocations have clearly interacted strongly with the cavities, either by intersecting them during propagation or nucleating on them. Close examination of images like Fig. 4 shows that the illuminated dislocation cores stop at the cavity edge, indicating that the cavity removes this highly strained material. The perimeters of many cavities are also highlighted by this contrast mechanism, and in some case, the entire cavity disk is illuminated, but these strains introduced around cavities are certainly confined to within less than one additional radius. These features agree with the theoretical finding of a small (2x), short-range correction to strain fields around cavities and support the approximations used to model more complex cavity configurations.

Table I. Relaxation of strained $Si_{0.86}Ge_{0.14}$/Si.

Anneal: Implant	1 hr. at 900°C	1 hr. at 1000°C	4 hr. at 1000°C
Unimplanted	< 1%	20-69%	43%
1.7×10^{16} He/cm^2	54%	81%	79%
4×10^{16} He/cm^2	68%	81%	

Table I gives relaxation values for the unimplanted reference and two implanted specimens after anneals at 900 or 1000°C. The values at 1000°C for the implanted specimens exceed that predicted for the $Si_{0.86}Ge_{0.14}$ alloy at thermal equilibrium [11], 76%. Analysis of Fig. 4 indicates that the fractional length of dislocation cores intercepted by cavities is ≈1/5. If the misfit-dislocation energy is correspondingly reduced by 1/5, the equilibrium relaxation increases to 80%, in agreement with our maximum values.

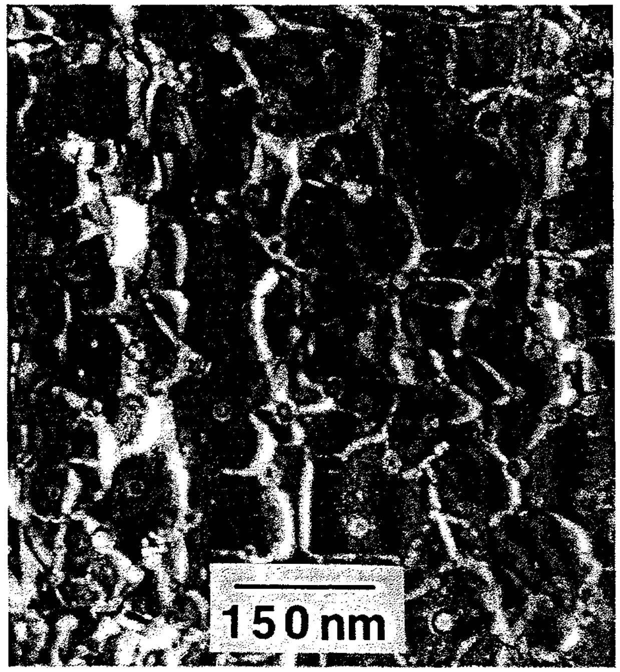

Figure 4. Weak-beam image of cavities and misfit dislocations in He-implanted $Si_{0.86}Ge_{0.14}$/Si after 1 hr. at 900°C.

InGaAs/GaAs HETEROSTRUCTURES

We previously developed a method to extend cavity formation to GaAs based on elevated-temperature implantations of Ar followed by He [3]. The Ar stabilizes lattice damage to provide nucleation sites for He bubbles. The elevated-temperature He implantation allows bubbles to coarsen and He to outgas while keeping the material intact, whereas room-temperature implantation and subsequent annealing produce surface blistering. We have applied this method to an $In_{0.10}Ga_{0.90}As$/GaAs heterostructure. A 330-nm alloy layer was grown by MBE at 530°C on (001) GaAs. The as-grown structure was 56% relaxed and showed misfit dislocations at the interface, along with dislocations extending into the substrate as in the SiGe/Si heterostructure [4]. Threading dislocations were not seen in the overlayer by cross-section TEM.

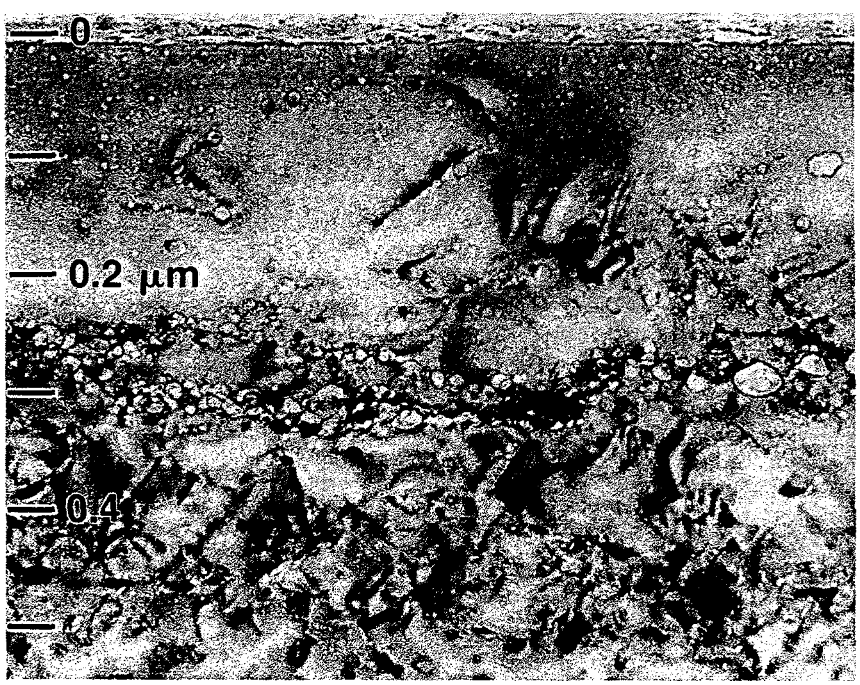

Figure 5. Cavities and defects in implanted $In_{0.10}Ga_{0.90}As$/GaAs.

Cavities were formed by implanting 1×10^{16} Ar/cm^2 at 360 keV and then 5×10^{16} He/cm^2 at 50 keV, both at 400°C. The microstructure is seen in the [110] cross section image in Fig. 5, obtained by underfocusing to highlight cavities while retaining some diffraction contrast to show lattice damage. A high density of cavities ~4-40 nm in diameter is seen near the interface, often dividing into multiple rows along dislocations that wander from the interface into the overlayer. In some cases the cavities are nearly contiguous and about to form cracks, which were observed in other regions. The alloy has many dislocations with 4-20 nm cavities, but also contains a uniform distribution of small ~2-5 nm cavities not on a dislocation. The GaAs substrate contains dislocations lying in {111} planes; close examination shows small ~3 nm cavities along them, as well as in the matrix. Small dislocation loops 8-20 nm across are seen at the deepest part of the implanted zone. These substrate features were also seen in GaAs given the same treatment [3].

The high density of small cavities in the alloy and substrate is believed due to numerous nucleation sites provided by the implanted Ar atoms and their lattice damage. The larger cavities (>10 nm) in the alloy are usually located on dislocations, and indicate an increased attraction due to their larger size. The high density of larger cavities on dislocations near the interface may be due to nucleation and growth on the misfit dislocations present in the original heterostructure. Such cavities either became bound to the dislocations, or nucleated on them and grew to larger sizes because dislocations are low-energy sites. In this system, the implantation at 400°C did not increase relaxation. The residual in-plane strain of -0.30% may be insufficient to propagate dislocations through the cavities and associated lattice damage. Enhanced dislocation nucleation is probably unimportant since the layer was already >50% relaxed.

DISCUSSION AND FURTHER IMPLICATIONS

The observations and calculations discussed above indicate that cavities are attracted to dislocations and bind strongly when the core passes through them. The large binding energy, ~800 eV for a 10 nm-radius cavity in Si, is put into perspective by noting that this volume would contain ~200,000 atoms. The normalized energy, ~0.004 eV/atom, is a modest value for a strain energy. The interaction is of relatively short range; a few radii from a dislocation the energy falls as $1/R_{dis}^2$ and the attractive force (energy gradient) as $1/R_{dis}^3$. Cavities intersecting a dislocation are thus likely to remain bound, but those separated by many radii are not likely to migrate to it.

An appropriately tailored cavity layer can be used to increase the strain relaxation rate of SiGe/Si heterostructures, and appears to alter the final equilibrium. As an additional means to manipulate strain and dislocations in a heterostructure, He can be implanted in situ during MBE growth to form cavities at the interface [5]. Cavities were observed to bind to dislocations in our initial attempt to alter relaxation of an InGaAs/GaAs heterostructure, but strain was unaffected and a high density of defects was introduced by the Ar implantation used to nucleate He bubbles.

The attractive interaction of cavities and dislocations is expected to occur in all crystalline solids, and was found in an early investigation of inert gas implantation into PbI_2 [12]. We note two examples found in our work on other materials. Recently, TEM was used to investigate hexagonal GaN grown on sapphire by metal-organic chemical vapor deposition [13]. A 50 nm layer of GaN was nucleated at 450°C and growth was initiated while ramping the temperature to 1030°C, where a 1.1 μm-thick layer was grown. The cross-section image in Fig. 6, obtained with reduced (0002) diffraction contrast and underfocusing to highlight cavities, shows near-vertical dislocations that have a screw displacement component and two tubular cavities along a section of the dislocation cores. As in SiGe, the cavity appears simply to remove the dislocation strain contrast that would have been seen. These tubes have diameters of 5-12 nm and are found with an areal density of ~$6x10^8/cm^2$; this is much higher than the tubes found by others [14] to extend entirely through GaN layers. In our material, tubes start and stop within the layer and are

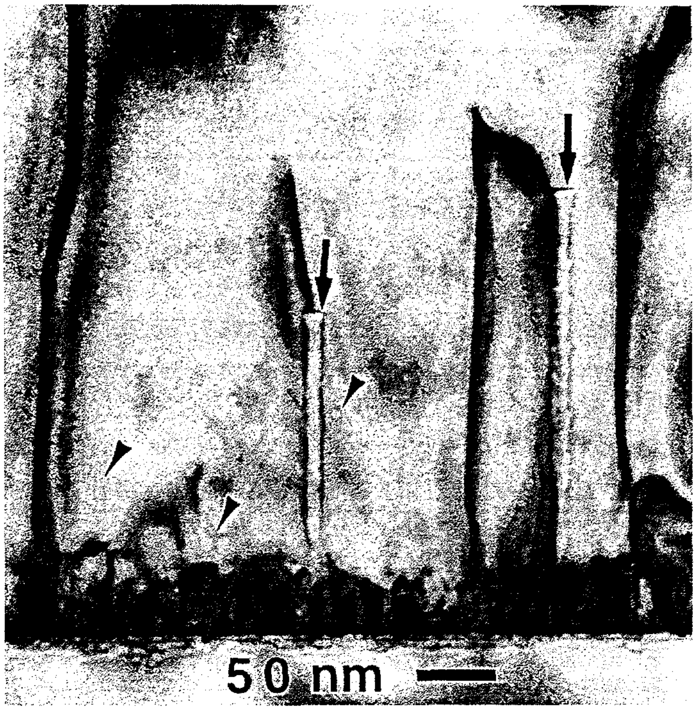

Figure 6. Tubular voids (large arrows) along cores of dislocations in GaN and other small voids (small arrows).

found near the interface as well as in the middle of the layer. The image also shows other small voids. We infer that the voids migrated to the dislocation cores during the high-temperature growth and formed the tubes. The tubular shape may possibly reflect a high dislocation core energy for GaN.

A second example is the microstructure of bubbles formed in He-implanted Fe [15]. After annealing to coarsen the bubbles, larger ones with diameters 5-9 nm are found along dislocation lines, whereas smaller bubbles are uniformly dispersed across the implanted layer. As discussed above, this indicates an attraction between the bubbles and dislocations. The interaction is expected in other metals including reactor alloys where He is introduced by nuclear reactions.

ACKNOWLEDGMENTS

The authors thank M. P. Moran for TEM technical support and imaging, and G. A. Petersen for performing the ion implantations. This work was supported by the U. S. Department of Energy under contract DE-AC04-94AL85000. Sandia is a multiprogram laboratory operated by Sandia Corporation, a Lockheed Martin company for the U. S. Department of Energy.

REFERENCES

1. C. C. Griffioen, J. H. Evans, P. C. de Jong and A. Van Veen, Nucl. Inst. Meth. **B27**, 417 (1987).
2. S. M. Myers, D. M. Follstaedt, H. J. Stein and W. R. Wampler, Phys. Rev. **B47**, 13 380 (1993).
3. D. M. Follstaedt, S. M. Myers, G. A. Petersen and J. C. Barbour, Mater. Res. Soc. Symp. Proc. **396**, 801 (1996).
4. D. M. Follstaedt, S. M. Myers and S. R. Lee, Appl. Phys. Lett. **69**, 2059 (1996).
5. D. M. Follstaedt, S. M. Myers, J. A. Floro and S. R. Lee, Nucl. Inst. Meth. B, in press.
6. S. M. Myers, unpublished work.
7. Specimen grown as in B. S. Myerson, Appl. Phys. Lett. **48**, 797 (1986).
8. D. M. Follstaedt, S. M. Myers, G. A. Petersen and J. W. Medernach, J. Electron. Mater. **25**, 151 (1996).
9. R. Hull, J. C. Bean, J. M. Bonar, G. S. Higashi, K. T. Short, H. Temkin and A. E. White, Appl. Phys. Lett. **56**, 2445 (1990).
10. F. LeGoues, K. Eberl and S. S. Iyer, Appl. Phys. Lett. **60**, 2862 (1992).
11. J. Y. Tsao, *Materials Fundamentals for Molecular Beam Epitaxy* (Academic, Boston, 1993).
12. A. J. Forty, in *Dislocations in Solids* (The Faraday Society, London, 1964), Vol. **38**, p. 56.
13. D. M. Follstaedt, J. Han, R. M. Biefeld and M. Weckwerth, unpublished work.
14. W. Qian, G. S. Rohrer, M. Skowronski, K. Doverspike, L. B. Rowland and D. K. Gaskill, Appl. Phys. Lett. **67**, 2284 (1995).
15. D. M. Follstaedt and S. M. Myers, *40th Ann. Proc. Electron Microscopy Soc. America* (San Francisco Press, 1982), p. 590.